KINEMATICS OF HYPER-REDUNDANT MANIPULATORS

Gregory S. Chirikjian and Joel W. Burdick
School of Engineering and Applied Science
California Institute of Technology
Pasadena, California

Abstract

A "hyper-redundant" manipulator is a redundant manipulator with a large or possibly infinite relative degree of redundancy. These manipulators are analogous in morphology to snakes, elephant trunks, and tentacles. This paper presents a novel approach to the forward and inverse kinematics of these manipulators which is based on differential geometry. The mechanisms are assigned a 'backbone curve' which captures the essential geometric features. A modal expansion of the backbone curve's curvature function is introduced in order to reduce the inverse kinematics problem to the search for a finite set of modal participation factors. For truly flexible devices, solutions derived from the backbone curve can be used directly to control the hyper-redundant arm geometry. For discrete linked manipulators, the actual manipulator is 'fitted' to the backbone curve solution.

1. Introduction

Hyper-redundant manipulators have a relative degree of redundancy which is large or infinite. In operation, these manipulators approximate the shape of snakes, elephants' trunks, or tentacles. Implementations of hyper-redundant manipulators may consist of truly flexible physical structures, such as a pneumatically driven hose, or consist of a large number of rigid links which approximate a continuous morphology. Several overviews and designs of hyper-redundant manipulators can be found in the robotics literature. It would seem that there are as many different names for these manipulators as there are authors. 'Hyper-redundant' manipulators have been called 'spine' [5], 'flexible' [7], 'tentacle' [8], 'elephant-trunk' [9], 'tensor-arm' [11], and 'snake-like'[12]. The hyper-redundant manipulator literature has primarily focused on manipulator systems, although one can also imagine using hyper-redundant mechanisms as grasping devices [10], or even for novel forms of locomotion [4]. Applications of hyper-redundant manipulators may include actively controlled medical endoscopes, devices to inspect pipes or tunnels, novel locomotion devices, and articulated space structures.

There has been a sporadic history of hyper-redundant manipulator research with few sustained efforts leading to practical results. The failure of hyper-redundant manipulators to achieve wide-spread applications is due to inefficiency and ineffectiveness of previous kinematic modeling techniques, complex mechanical design, and complexity in the programming of these devices arising from their non-anthropomorphic geometry. In this paper we address the first problem. Novel and efficient techniques and algorithms for analyzing the forward and inverse kinematics of hyper-redundant manipulators are presented. It is hoped that this framework will form a foundation for future work which will enable hyper-redundant manipulators to be more widely applied. Related works in obstacle avoidance and locomotion which employ this basic framework can be found in [2,4].

2. Differential Geometry of Planar Curves

A planar hyper-redundant manipulator may be comprised of many rigid links, as in Figure 1(a), or the physical construction of the device may be truly flexible–such as a pneumatic or tendon based structure, as in Figure 1(b). This section will consider only the case of continuous planar manipulators, as Section 6 explains how this analysis can be extended to the case of rigid link manipulators.

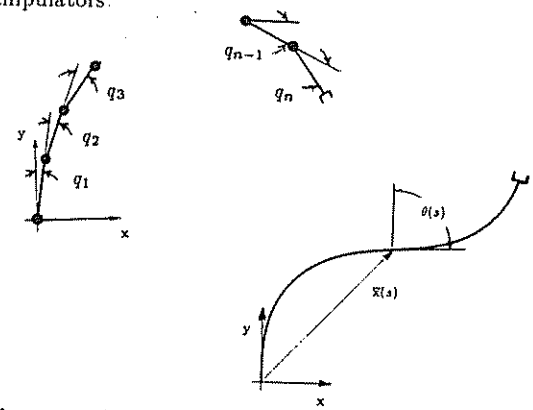

Figure 1: Planar Hyper-Redundant Manipulators

We assume that the geometric features of a hyper-redundant manipulator can be captured by a "backbone curve," of constant length, which lies along the centerline of the hyper-redundant manipulator. Attach a frame defining an x_1-x_2 coordinate system to the base of the backbone curve. The 'backbone curve' is the locus of all points in the base frame which have position defined by $\overline{x}(s) = [x_1(s),\ x_2(s)]^T$. s is the backbone curve arc length, measured from the origin, and it is assumed that all lengths in the plane are scaled to units of the constant manipulator length so that s is in the range $0 \leq s \leq 1$. It is possible to define a single function, the *curvature function*, defined as $\kappa(s) = |d^2\overline{x}/ds^2|$, which totally defines the shape of a planar curve.

If we assume that $\overline{x}(0) = \overline{0}$ and that the tangent to the backbone curve at its base point is in the x_2-direction ($d\overline{x}/ds = [0\ 1]^T$), the curve can be parameterized as follows:

$$x_1(s) = \int_0^s \sin\theta(\sigma)d\sigma \qquad x_2(s) = \int_0^s \cos\theta(\sigma)d\sigma \qquad (1)$$

where:

$$\theta(s) = \int_0^s \kappa(\sigma)d\sigma \qquad (2)$$

$\theta(s_0)$ is the angle which the tangent to the curve at $s = s_0$ makes with the tangent at the point $s = 0$ (the x_2-axis) measured clockwise. This formulation is not altered if the curvature function depends upon time as well as arclength.

> **Remark:** Planar hyper-redundant manipulator forward kinematics is completely determined by the curvature function of the backbone curve. In this approach, hyper-redundant manipulator inverse kinematics and trajectory planning operations are reduced to finding the proper time varying behavior of the curvature function so as to induce the desired manipulator behavior. That is, the function $\kappa(s,t)$ will determine the bending of the manipulator as a function of time, and is selected to achieve desired objectives, which depend upon the nature of the hyper-redundant manipulator application.

3. Planar Hyper-Redundant Kinematics

This section presents one method, based on a modal expansion of the curvature function, for making the inverse kinematics of manipulator backbone curves tractable. This method could be used for trajectory planning purposes in the same way that inverse kinematics algorithms are used as the basis for planning joint trajectories of non-redundant manipulators. Forward kinematics can be computed by exact or numerical integration of (1). However, the inverse kinematic problem would essentially be a blind search for curvature functions which satisfy the forward kinematic constraints. Each guess would involve integration of (1), and such a procedure would require numerous computations, limiting the applicability of this approach.

However, the complexity of the inverse kinematic problem can be reduced by limiting the curvature functions to a modal form:

$$\kappa(s,t) = \sum_{i=1}^{N} a_i(t)\phi_i(s), \qquad (3)$$

where $\phi_i(s)$ is a *curvature mode function*, and a_i is termed a *modal participation factor*. N is the number of modes, which will depend upon the number of kinematic constraints which are specified.

The curvature modes are specified functions, and thus the inverse kinematics problem is reduced to finding the $\{a_i\}$ which satisfy the end effector constraints. For some choices of modes, exact inverse kinematic solutions can be found, some of which are presented below. In general the $\{a_i\}$ must be found numerically. The greatest benefit of the modal approach is that N, the number of modes, can be chosen to be significantly less than n, the number of manipulator degrees of freedom. This leads to considerable savings in inverse kinematics computations.

3.1. Closed Form Examples

Consider the following choice of modes for $N = 2$*:

$$\phi_1(s) = 2\pi\cos 2\pi s; \qquad \phi_2(s) = 2\pi\sin 2\pi s. \qquad (4)$$

Substituting these two modes into (1-3), it can be shown [1] that the forward kinematics equations reduce to

$$x_1(1) = \sin(a_2)J_0\left[(a_1^2 + a_2^2)^{\frac{1}{2}}\right] \qquad x_2(1) = \cos(a_2)J_0\left[(a_1^2 + a_2^2)^{\frac{1}{2}}\right] \qquad (5)$$

where J_0 is the zeroth order Bessel function. Henceforth the notation $x_{ee} = x_1(1)$ and $y_{ee} = x_2(1)$ is used. The 'inverse kinematics' (evaluation of modal participation factors) in this case can be computed as:

$$a_2 = \text{Atan2}\,(x_{ee}, y_{ee}) \qquad (6.a)$$

$$a_1 = \pm\left(\left[J_0^{-1}\left[(x_{ee}^2 + y_{ee}^2)^{\frac{1}{2}}\right]\right]^2 - [\text{Atan2}\,(x_{ee}, y_{ee})]^2\right)^{\frac{1}{2}}. \qquad (6.b)$$

J_0^{-1} is the 'restricted inverse Bessel function of zero order', and is defined as the inverse of $J_0(x)$ for $0 < x < \mu$ where $\mu \approx 3.832$ is the first local minimum of J_0. J_0 is monotonically decreasing over $(0, \mu)$, and there is no problem in defining a unique inverse. If the J_0 were not restricted to this interval, multiple solutions would be possible. The higher order solutions would physically correspond to self-intersecting configurations of the manipulator, and these solutions are neglected on the basis of practical considerations.

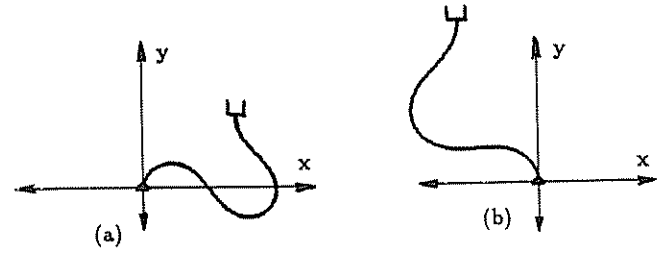

Figure 2: One Possible Choice of Modes

* These modes were chosen solely because they lead to a closed form inverse kinematic solution

Figures 2(a) and 2(b) show two examples of the inverse kinematic solutions provided by (6). In Figure 2(a), the manipulator end-effector is commanded to move to location $(x_{ee}, y_{ee}) = (0.3433, 0.2733)$. From (6), the modal participation factor solutions are $a_1 = 1.3588$ and $a_2 = 0.8984$. Figure 2(b) is another example with $(x_{ee}, y_{ee}) = (-0.2933, 0.6133)$, which results in modal participation factors of $a_1 = -1.0957$, $a_2 = -0.4461$.

Of the other closed form solutions which have been found, the following are among the simplest. If we take

$$\phi_1(s) = 2\pi\cos(2\pi s); \qquad \phi_2(s) = \delta(s - 0^+)$$

where δ represents a delta function, the forward kinematics can be written:

$$x_{ee} = J_0(a_1)\sin a_2; \qquad y_{ee} = J_0(a_1)\cos a_2.$$

The inverse kinematics is then

$$a_1 = J_0^{-1}((x_{ee}^2 + y_{ee}^2)^{\frac{1}{2}}); \qquad a_2 = \mathrm{Atan2}(x_{ee}, y_{ee})$$

Similarly, if we take

$$\phi_1(s) = 2\pi\sin(2\pi s); \qquad \phi_2(s) = \delta(s - 0^+)$$

the forward kinematics becomes

$$x_{ee} = J_0(a_1)\sin(a_1 + a_2); \qquad y_{ee} = J_0(a_1)\cos(a_1 + a_2)$$

and the inverse kinematics is

$$a_1 = J_0^{-1}((x_{ee}^2 + y_{ee}^2)^{\frac{1}{2}}); \qquad a_2 = \mathrm{Atan2}(x_{ee}, y_{ee}) - a_1.$$

3.2 Modal Singularities and Mode Switching

While the introduction of modes reduces computational needs, it also introduces new problems, such as modal singularities. Modal singularities are analogous to the kinematic singularities of standard manipulators. In a standard kinematic singularity, an instantaneous motion of the joints is unable to provide an instantaneous motion of the end-effector in one or more directions in the workspace. For modal singularities, the loss of end-effector freedom is measured with respect to instantaneous changes in modal participation factors. The Jacobian matrix is defined as:

$$\mathbf{J}_{ik} = \frac{\partial x_i}{\partial a_k}. \tag{7}$$

To illustrate modal singularities (7) is evaluated with the choice of modes given by Equation (4). Since two participation factors are involved, and we are only interested in end-effector position in the plane, loss of rank can be determined by setting

$$|\mathbf{J}| = \frac{\partial x_{ee}}{\partial a_1}\frac{\partial y_{ee}}{\partial a_2} - \frac{\partial x_{ee}}{\partial a_2}\frac{\partial y_{ee}}{\partial a_1} = 0. \tag{8}$$

Substituting (5) into (8), the modal singularities of this manipulator occur when:

$$a_1(a_1^2 + a_2^2)^{\frac{1}{2}} J_1\left[(a_1^2 + a_2^2)^{\frac{1}{2}}\right] J_0\left[(a_1^2 + a_2^2)^{\frac{1}{2}}\right] = 0. \tag{9}$$

Equation (9) will be satisfied for any one of the following conditions: $a_1 = 0$, $J_0\left[(a_1^2 + a_2^2)^{\frac{1}{2}}\right] = 0$, or $J_1\left[(a_1^2 + a_2^2)^{\frac{1}{2}}\right] = 0$. The case of $a_1 = 0$ corresponds to the workspace boundary, and physically means that for this set of modes the manipulator can not extend further in a direction normal to the boundary imposed by these modes. The other conditions occur when $(a_1^2 + a_2^2)^{\frac{1}{2}}$ is a zero of either of the functions J_0 or J_1. Since the inverse kinematics solution uses a restricted Bessel function, the only time this happens is when $(a_1^2 + a_2^2)^{\frac{1}{2}} = \mu_1$ where $\mu_1 \simeq 2.405$ is the first zero of J_0.

Figure 3(a) shows the a_1-a_2 modal participation factor space for this choice of modes and the loci of a_1 and a_2 values which lead to modal singularities. Figure 3(b) shows the loci of end-effector positions where modal singularities occur.

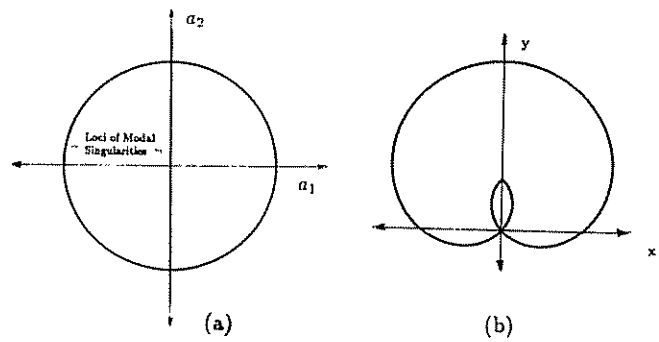

Figure 3: Loci of Modal Singularities

Care must be exercised in choosing curvature mode functions to avoid *degenerate* mode choices. For example, if the $\{\phi_i\}$ are chosen to be linearly dependent, the number of end-effector degrees of freedom will be less than the number of modal participation factors for all values. Consequently, linear independence is a necessary condition for a choice of modes to be nondegenerate. However, linear independence is not a sufficient condition. For instance, it can be shown [1] that if all the ϕ_i's are chosen to be functions which are even about the point $s = \frac{1}{2}$, with zero mean value over the interval $0 \le s \le 1$, the hyper-redundant manipulator end-effector will be constrained to move along the x_2-axis for all values of $\{a_i\}$, even though the modes are linearly independent. Thus a stronger condition than linear independence of mode functions is necessary.

> **Definition:** A choice of modes is *degenerate* if J loses rank for all values of modal participation factors. A set of modes can be tested for degeneracy by simply evaluating the rank of the Jacobian for a random selection of $\{a_i\}$. If the Jacobian is full rank for any set of $\{a_i\}$, the modes are nondegenerate.

The introduction of modes may restrict the manipulator to operate in a workspace which is smaller than dictated by physical limitations on the manipulator. However, the potential to switch among several sets of modes allows this approach to cover the workspace of the manipulator. Figure 4 shows a schematic picture of a manipulator's physical workspace which is "covered" by different overlapping modal regions.

To smoothly switch from a set of modes $\{\phi_i^I\}$ to the set $\{\phi_i^O\}$ the curvature function will be of the form

$$\kappa(s,t) = \sum_{i=1}^{N}\left[a_i^I(t)\phi_i^I(s) + a_i^O(t)\phi_i^O(s)\right] \tag{10}$$

where at the beginning of the switching process, which we denote by $t = 0$, $a_i^O(0) = 0$ for all $i \in [1, N]$ and at the end of the process, denoted by $t = 1$, $a_i^I(1) = 0$ for all $i \in [1, N]$. If the end-effector must remain stationary during the procedure, the following relation can be used to control the mode switching:

$$\mathbf{J}_I \dot{\overline{a}}^I + \mathbf{J}_O \dot{\overline{a}}^O = \overline{0} \tag{11}$$

$\mathbf{J}_I$ and $\mathbf{J}_O$ are the Jacobians associated with the original and new participation factors. One of the two Jacobians need be full rank for (11) to be useful. By defining $\overline{a}^O$ to be an increasing function of time and inverting $\mathbf{J}_I$, $\dot{\overline{a}}^I$ can be found. Conversely, by defining $\overline{a}^I$ to be a decreasing function of time and inverting $\mathbf{J}_O$, $\dot{\overline{a}}^O$ can be found. If both Jacobians are singular, the constraint of constant end effector position as a function of time must be relaxed.

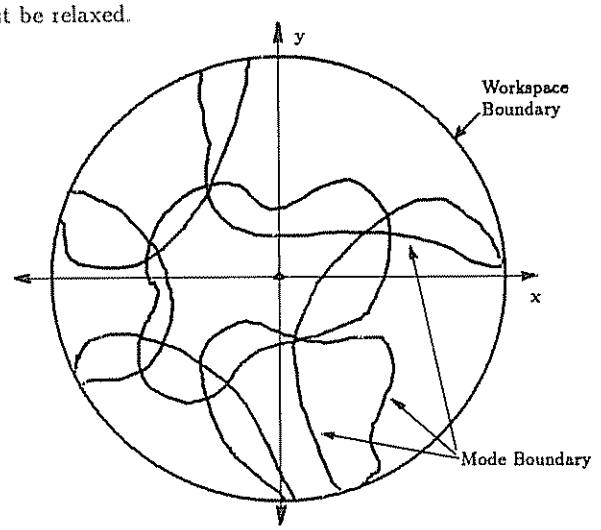

Figure 4: Multiple Mode Covering of the Workspace

4. Representation of Space-Curves

Given a space curve parametrized by arclength, s, with position vector to every point on the curve $\overline{x}(s)$, a parameter called torsion, $\tau(s)$, is needed in addition to curvature, $\kappa(s)$, to uniquely specify a space curve. The classical definitions of curvature and torsion are

$$\kappa^2 = \overline{x}'' \cdot \overline{x}'' \qquad \tau = \overline{x}' \cdot \left(\overline{x}'' \times \overline{x}'''\right) / \kappa^2 \tag{12}$$

where a $'$ represents a derivative with respect to s. A unique frame, termed the Frenet-Serret frame, can be assigned to the curve at all points for which κ and τ are not zero. This frame is denoted by the triplet of vectors $\{\overline{\Phi}_1(s), \overline{\Phi}_2(s), \overline{\Phi}_3(s)\}$, where:

$$\overline{\Phi}_1 = \overline{x}'; \qquad \overline{\Phi}_2 = \overline{x}''/\kappa; \qquad \overline{\Phi}_3 = \left(\overline{x}' \times \overline{x}''\right)/\kappa \tag{13}$$

are respectively called the tangent, normal, and binormal.

To date there is no spatial analogue to the convenient planar equations (1) which relates the parameters κ and τ to the position of all points on the curve. However, it is possible to define functions of arclength other than curvature and torsion which are more convenient to describe the geometry of a space curve. Here we use quantities which we refer to as *quasi-curvature* and *quasi-torsion* denoted by the letters $\mathcal{K}$ and $\mathcal{T}$ respectively. Defining

$$K(s) = \int_0^s \mathcal{K}(\sigma)d\sigma \qquad T(s) = \int_0^s \mathcal{T}(\sigma)d\sigma \tag{14}$$

every point on the space curve can be represented by the parametric equations:

$$\overline{x}(s) = \begin{pmatrix} \int_0^s \sin K(\sigma)\cos T(\sigma)d\sigma \\ \int_0^s \cos K(\sigma)\cos T(\sigma)d\sigma \\ \int_0^s \sin T(\sigma)d\sigma \end{pmatrix} \tag{15}$$

This form is not unique and was chosen so that the conditions at $s = 0$ on the curve are the same as the planar case, $\overline{x}(0) = \overline{0}$; $\overline{x}'(0) = [0\ 1\ 0]^T$. The functions K and T can be related back to curvature and torsion through the relationships:

$$\kappa^2 = (T')^2 + (K')^2 \cos^2 T \tag{16}$$

$$\tau = -K' \sin T + \frac{1}{\kappa^2}\left[(T'K'' - T''K')\cos T - (T')^2 K' \sin T\right] \tag{17}$$

which can be derived from (12).

Like the classical parametrization of space curves, a frame can be assigned to every point on a space-curve defined by the parameters K, and T. This frame is denoted by the triplet of vectors $\{\overline{\Psi}_1(s), \overline{\Psi}_2(s), \overline{\Psi}_3(s)\}$ which have the explicit representation:

$$\overline{\Psi}_1 = \begin{pmatrix} \sin K \cos T \\ \cos K \cos T \\ \sin T \end{pmatrix}; \overline{\Psi}_2 = \begin{pmatrix} -\sin K \sin T \\ -\cos K \sin T \\ \cos T \end{pmatrix}; \overline{\Psi}_3 = \begin{pmatrix} \cos K \\ -\sin K \\ 0 \end{pmatrix} \tag{18}$$

and are referred to as the *tangent*, *complementary* vector, and *planar-normal* respectively. This frame relates back to the Frenet frame through a rotation about the tangent vector:

$$\Phi_i(s) = \mathrm{ROT}[\Psi_1(s), \beta(s)]\Psi_i(s)$$

where $\beta = \mathrm{Atan2}(T', K' \cos T)$. Parametrization of space curves with $\mathcal{K}$ and $\mathcal{T}$ has other advantages besides the existence of an easily defined frame. The initial conditions at the base of the spatial curve are easily specified in this framework, and this parameterization allows closed form solutions based on the same approach used in the planar case. The price to pay for this simplicity is that in some sense the 'intrinsicness' of the formulation has been lost.

To recognize the similarity in mathematical form between the spatial and the planar cases, use the relationships:

$$\sin K \cos T = \frac{1}{2}[\sin(K+T) + \sin(K-T)]$$
$$\cos K \cos T = \frac{1}{2}[\cos(K+T) + \cos(K-T)]$$

to write the equations for the position of the end-effector of the curve as

$$\int_0^1 \sin\theta^+ ds + \int_0^1 \sin\theta^- ds = 2x_1(1) = 2x_{ee} \tag{19a}$$

$$\int_0^1 \cos\theta^+ ds + \int_0^1 \cos\theta^- ds = 2x_2(1) = 2y_{ee} \tag{19b}$$

$$\int_0^1 \sin\frac{1}{2}(\theta^+ - \theta^-)ds = x_3(1) = z_{ee} \qquad (19c)$$

where

$$\theta^+(s) = K(s) + T(s); \qquad \theta^-(s) = K(s) - T(s).$$

Thus the geometry of space curves can be represented as 'coupled' planar problems.

5. Spatial Hyper-Redundant Manipulators

The modal method can be used to formulate algorithms for spatial hyper-redundant manipulators. Let

$$\mathcal{K}(s) = \sum_{i=1}^{N_K} a_i\phi_i(s); \qquad \mathcal{T}(s) = \sum_{i=1}^{N_T} \alpha_i\xi_i(s). \qquad (20)$$

where a_i and α_i can vary with time as the end-effector moves. However, unlike the planar case, the curve representation of hyper-redundant manipulators is not sufficient. A third quantity $\mathcal{R}(s)$, termed the *rate of roll distribution* must be defined such that

$$R(s) = \int_0^s \mathcal{R}(\sigma)d\sigma \qquad (21)$$

where $R(s)$ is the roll of all points along the manipulator with respect to the reference frame $\{\Psi_i\}$ and is measured in the plane normal to the tangent to the curve. $\mathcal{R}(s)$ can be expanded in a modal form in the same way that $\mathcal{K}(s)$ and $\mathcal{T}(s)$ were.

Thus if the end effector orientation is specified by a vector of direction cosines $\overline{\gamma} = [\gamma_1, \gamma_2, \gamma_3]^T$ and a roll ρ measured with respect to the frame $\{\Psi_i\}$, the conditions which must be satisfied are

$$\begin{aligned} \sin\theta^+(1) + \sin\theta^-(1) &= 2\gamma_1 \\ \cos\theta^+(1) + \cos\theta^-(1) &= 2\gamma_2 \end{aligned} \qquad (22a)$$

$$\sin\frac{1}{2}(\theta^+(1) - \theta^-(1)) = \gamma_3 \qquad (22b)$$

$$R(1) = \rho \qquad (22c)$$

Note that equations (22a) are equivalent to the forward kinematics equations of a two link revolute-jointed planar manipulator with unit length links, and the solution to that problem can be used to calculate two solutions to (22a):

$$\begin{aligned} \theta^-(1) &= \mathrm{Atan2}(\gamma_1, \gamma_2) - \mathrm{Atan2}\left(\gamma_3(1-\gamma_3^2)^{\frac{1}{2}}, 1-\gamma_3^2\right) \\ \theta^+(1) &= \theta^-(1) + \mathrm{Atan2}\left(2\gamma_3(1-\gamma_3^2)^{\frac{1}{2}}, 1-2\gamma_3^2\right). \end{aligned} \qquad (23a)$$

$$\begin{aligned} \theta^-(1) &= \mathrm{Atan2}(\gamma_1, \gamma_2) - \mathrm{Atan2}\left(-\gamma_3(1-\gamma_3^2)^{\frac{1}{2}}, 1-\gamma_3^2\right) \\ \theta^+(1) &= \theta^-(1) + \mathrm{Atan2}\left(-2\gamma_3(1-\gamma_3^2)^{\frac{1}{2}}, 1-2\gamma_3^2\right). \end{aligned} \qquad (23b)$$

It can also be shown that equation (22b) is automatically satisfied by the solutions of (23a,b). Equation (22c) is solved independently of the other equations. Determination of appropriate modal participation factors for a given orientation is a linear problem from this point.

At least 5 unknown modal participation factors, distributed between $\{a_i\}$ and $\{\alpha_i\}$, and at least a one parameter roll distribution are needed to solve spatial position and orientation problems using the methods outlined in this section. With the similarity between the two and three dimensional cases apparent, analysis of the planar case provides much of the necessary tools for solving spatial problems.

The closed form planar kinematics solutions can be applied to find closed form forward kinematics equations for the three dimensional case. For instance, let:

$$\begin{aligned} \mathcal{K}(s,t) &= 2\pi a_1\cos 2\pi s + 2\pi a_2 \sin 2\pi s \\ \mathcal{T}(s,t) &= 2\pi a_3\cos 2\pi s + 2\pi a_4 \sin 2\pi s. \end{aligned} \qquad (24)$$

Since $\mathcal{K}$ and $\mathcal{T}$ act in different planes at every point along the manipulator they can be chosen to be similar functions without having to worry about linear dependence. The forward kinematic equations corresponding to these modes are:

$$\begin{aligned} x_{ee} &= \frac{1}{2}J_0[((a_1+a_3)^2 + (a_2+a_4)^2)^{\frac{1}{2}}]\sin(a_2+a_4) \\ &\quad + \frac{1}{2}J_0[((a_1-a_3)^2 + (a_2-a_4)^2)^{\frac{1}{2}}]\sin(a_2-a_4) \\ y_{ee} &= \frac{1}{2}J_0[((a_1+a_3)^2 + (a_2+a_4)^2)^{\frac{1}{2}}]\cos(a_2+a_4) \\ &\quad + \frac{1}{2}J_0[((a_1-a_3)^2 + (a_2-a_4)^2)^{\frac{1}{2}}]\cos(a_2-a_4) \\ z_{ee} &= J_0[(a_3^2 + a_4^2)^{\frac{1}{2}}]\sin a_4 \end{aligned} \qquad (25)$$

The authors have not found closed from inverse kinematic solutions for (25). However, the existence of closed form forward kinematic solutions makes rate formulations faster than if integrals would have to be computed at every time step.

6. Fitting a Discrete Manipulator

The continuous backbone curve approach presented earlier can be applied directly to control the geometry of actual hyper-redundant manipulators with a continuous morphology. However, in practice, many hyper-redundant manipulators might be constructed of a large number of discrete links, and the continuous inverse kinematic approach doesn't directly apply. This section demonstrates the adaptation of the modal method to the case of an n-link planar revolute manipulator. The primary assumption is that the discrete-linked manipulator has a sufficient number of degrees of freedom so that a continuous backbone curve inverse kinematic solution can be used to approximate the discrete link joint angles, or other pertinent parameters for the discrete actuators (such as tendons). Two methods of approximation are possible. In the first method, one is only concerned with guaranteeing that the end-effector of the discrete manipulator aligns with the end-effector of the continuous backbone curve manipulator. This method is computationally very efficient, and can be found in [1]. In the second and more complicated method which is summarized below, the discrete manipulator geometry is selected so that both the end-effector and the nominal shape of the discrete manipulator coincide as closely as possible with the continuous backbone curve solution. A more complete derivation of this methodology can be found in [1,2].

Figure 1(a) shows a planar manipulator comprised of n rigid links with n revolute joints. All links are assumed to be of the same length, and the total length of the manipulator is normalized to 1. It is also assumed that the backbone curve inverse

kinematic solution has been compute so that the $\{a_i\}$ are known for a given set of curvature modes $\{\phi_i\}$.

In this method, the joint angles, $\{q_j\}$ of the discrete manipulator are computed as:

$$q_{j+1} = \theta\left(\frac{2j+1}{2n}\right) - \theta\left(\frac{2j-1}{2n}\right) + \epsilon_{j+1} \tag{26}$$

In other words, we take the angles of the discrete case to be approximately the change in angle over a corresponding section of length in the continuous case. This approximation will lead to errors, and to account for these errors, we introduce n free 'fitting' parameters, $\{\epsilon_j\}$.

The $\{\epsilon_j\}$ are computed to minimize a function which is the sum of squared distance between points on both manipulators located at $s = \frac{i}{n}$ for $i = 1, \ldots, n$:

$$G = \frac{1}{2}\sum_{k=1}^{n}\left[\left(\int_0^{\frac{k}{n}} \sin\theta ds - \frac{1}{n}\sum_{i=1}^{k}\sin\sum_{j=1}^{i} q_j\right)^2 + \left(\int_0^{\frac{k}{n}} \cos\theta ds - \frac{1}{n}\sum_{i=1}^{k}\cos\sum_{j=1}^{i} q_j\right)^2\right]. \tag{27}$$

Assuming each ϵ_i is small, (27) can be linearized to provide n linear equations in the n unknown $\{\epsilon_i\}$. If the computed values of $\{\epsilon_i\}$ are small, the linearization assumptions are justified. If the $\{\epsilon_i\}$ are not sufficiently small, iteration of the above procedure or a nonlinear fitting technique can be used. This will generally only be the case when there are points on the backbone curve with large curvature magnitude. Such cases can be avoided by restricting the maximum curvature magnitude, possibly at the expense of reducing the volume of the workspace associated with a particular set of modes. Restrictions of the maximum curvature correspond to restrictions on the $\{a_i\}$, and are analogous to joint angle limits.

7. Conclusions

This paper presented a novel approach to the kinematic analysis of hyper-redundant robot manipulators. An associated "backbone curve," which captures the shape of the manipulator, was introduced to model the manipulator geometry. Differential geometry was used to develop the kinematic equations of the backbone curve. The kinematic analysis was simplified by introducing the *modal approach*, which leads to closed form forward and inverse kinematics solutions in some cases. In addition, methods for fitting the continuous backbone kinematic solutions to discrete manipulator structures were developed and applied to planar examples. An expression for modal singularities was developed, and the concept of mode switching for circumventing them was introduced. In companion works, we have used similar formulations to develop new methods for hyper-redundant manipulator obstacle avoidance [2], path planning [3], and locomotion [4].

8. References

[1] Chirikjian, G.S., Burdick, J.W., "A Modal Approach to the Kinematics of Hyper-Redundant Manipulators," *Robotics and Mechanical Systems Technical Report* No. RMS-89-3, Dept. of Mechanical Engineering, California Institute of Technology, Sept. 1989.

[2] Chirikjian, G.S., Burdick, J.W., "A Geometric Approach to Hyper-Redundant Manipulator Obstacle Avoidance," to appear in the *Proceedings of the ASME Mechanisms Conference*, Chicago, Il, Sept. 16-19, 1990.

[3] Chirikjian, G.S., Burdick, J.W., "Pseudo-Dynamics Algorithms for Computing Inverse Kinematics and Path Planning of Robotic Manipulators," *Robotics and Mechanical Systems Technical Report* No. RMS-89-5, Dept. of Mechanical Engineering, California Institute of Technology, March 1990.

[4] Chirikjian, G.S., Burdick, J.W., "Hyper-Redundant Robotic Locomotion: Locomotion Without Wheels Tracks, or Legs," *Robotics and Mechanical Systems Technical Report* No. RMS-89-6, Dept. of Mechanical Engineering, California Institute of Technology, March 1990.

[5] Drozda, T.S., "Spine Robot ... The Verdict's Yet to Come," *Manufacturing Engineering*, Vol. 93, No. 3, Sept. 1984, pp. 110-112.

[6] Hirose, S., Umetani, Y., "Kinematic Control of Active Cord Mechanism With Tactile Sensors," *Proceedings of Second International CISM-IFT Symposium on Theory and Practice of Robots and Manipulators*, pp. 241-252, 1976.

[7] Hemami, A.,"Studies on a Light Weight and Flexible Robot Manipulator," *Robotics*, Vol. 1, 1985, pp. 27-36.

[8] Ivanescu, M., Badea, I.,"Dynamic Control for a Tentacle Manipulator," Int. Conf. on Robotics and Factories of the Future, pp. 317-328, Dec 4-7, 1984, Charlotte, Nc, USA.

[9] Morecki, A., et al, "Robotic System - Elephant Trunk Type Elastic Manipulator combined with a Quadruped Walking Machine," *Proc. of Second Int. Conf. on Robotics and Factories of the Future*, San Diego, July 1987, pp. 649-656.

[10] Pettinato, J.S., Stephanou, H.E., "Manipulability and Stability of a Tentacle Based Robot Manipulator," *Proceedings of the 1989 IEEE International Conference on Robotics and Automation*, May 15-19, 1989, Scottsdale, AZ, pp. 458-463.

[11] Shahinpoor, M., Kalhor, H., Jamshidi, M., "On Magnetically Activated Robotic Tensor Arms," *Proceedings of the International Symposium on Robot Manipulators: Modeling, Control, and Education*, Nov. 12-14, 1986, Albuquerque, New Mexico.

[12] Tesar, D., Butler, M.S., "A Generalized Modular Architecture for Robot Structures," *ASME Manufacturing Review*, Vol. 2, No. 2, June 1989, pp. 91-118.